Estimation of $ZZ \rightarrow ll\nu\nu$ background using $Z(\rightarrow ll) + \gamma$ data

Mid Year Report - November 2017

Mangesh Sonawane

Supervisor: Dr. Beate Heinemann

June 2017 - May 2018

Contents

Abstract

In the search for Dark Matter at the LHC, SM particles are produced in association with DM particles, which are invisible as they don't interact with the detector. Thus events with large imbalance in transverse momentum are of interest. One such signature is $ll + E_T^{miss}$. *The dominant background contributing to the* $ll + E_T^{miss}$ *is* $ZZ \rightarrow ll\nu\nu$. *Currently, this background is determined using Monte Carlo simulation, with an uncertainty of* $\approx 10\%$ *[1]. The goal of this study is to establish a data driven method to estimate this background, and reduce the uncertainty. Using* $Z\gamma \rightarrow ll\gamma$ *, which is a pure signal and has a high* $BR * \sigma$, *it is possible to obtain the* $ZZ \rightarrow ll\nu\nu$ *contribution. In regions where* $p_T(\gamma) \gg M_Z$, *the two processes are kinematically similar. They have the same production mechanisms, but differ due to the photon and Z boson couplings to the quarks being different, as well as the difference in mass (photons are massless, while Z bosons are massive). Introducing a transfer factor R, as the ratio* $\sigma(ZZ)/\sigma(Z\gamma)$ *which is determined by simulation, the contribution of* $ZZ \rightarrow ll\nu\nu$ *to the background can be estimated from* $Z\gamma \rightarrow ll\gamma$ *data.*

1 Introduction

Among the candidates for Dark Matter at the LHC are WIMPs (Weakly Interacting Massive Particles). The signature for WIMPs are events with large missing transverse momentum $E_T^{miss} = -(\sum p_T)$, where the sum is taken over all tracks. One such signal we look at is $ll + E_T^{miss}$. WIMPs do not register in the detector, and thus result in a large missing transverse momentum (also referred to here as MET).
For example, the production of Higgs in association with a Z, as shown in Fig.1, is one possible process giving the $ll + E_T^{miss}$ signature, if the mass of the DM particle is less than half the mass of the Higgs Boson.

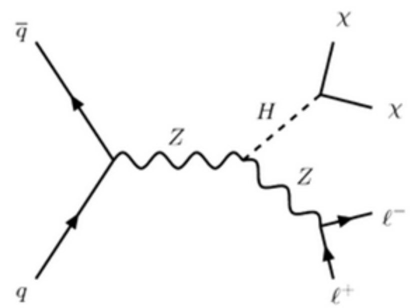

Figure 1: Feynman diagram showing the associated production of Higgs. The Higgs boson decays to two invisible DM particles and the Z boson decays leptonically, resulting in the $ll + E_T^{miss}$ signature.

The background processes are $ZZ \rightarrow ll\nu\nu$, $WZ \rightarrow lll\nu$,$WW \rightarrow l\nu l\nu$, Z+jets and W+jets. The dominant source of background is the $ZZ \rightarrow ll\nu\nu$ process, contributing $\approx 60\%$ of the background. Figure 2 shows the production modes of ZZ from $q\bar{q}$ and gg scattering.
A precise estimate of this process, along with the uncertainty associated with it, is crucial. In current analyses, this is determined using simulation, with an uncertainty of $\approx 10\%$ [1].

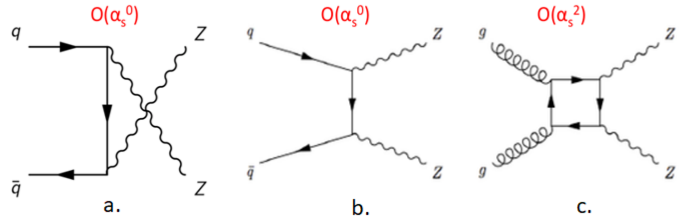

Figure 2: Feynman Diagram showing ZZ Production
a. & b. $q\bar{q} \to ZZ$ c. $gg \to ZZ$

One method of estimating this contribution is to look at $ZZ \to llll$, which has a branching fraction of $\approx 0.46\%$. This is due to the low branching fraction of $Z \to ll$ [1], and is thus statistically limited. Only electrons and muons are considered here as the leptonic decay products of the Z bosons. In contrast, the branching fraction of $ZZ \to ll\nu\nu$ is 2.7%, about 6 times higher than $ZZ \to llll$.

As in earlier analysis that used γ+jets to calibrate Z+jets background [2], in the region where the mass of the Z boson is negligible to the tranverse momentum p_T, the $Z\gamma \to ll\gamma$ process should be kinematically similar to $ZZ \to ll\nu\nu$ as the mass of the Z boson is negligible. Figures 2 and 3 show the leading order Feynman diagrams for the production of ZZ and $Z+\gamma$ respectively. The diagrams for $q\bar{q}$ and gg (a. b. and c.) are similar. Diagram 3d. corresponds to the production of a single Z boson, with the photon radiated from a final state lepton.
In addition to having a higher $BR * \sigma$ as compared to $ZZ \to ll\nu\nu$ (2.7% for ZZ vs 6.8% for $Z\gamma$), the $Z\gamma \to ll\gamma$ signal is also very pure. Thus, it should be possible to use $Z\gamma \to ll\gamma$ data to estimate $ZZ \to ll\nu\nu$ contribution to the background, and obtain a more accurate prediction.

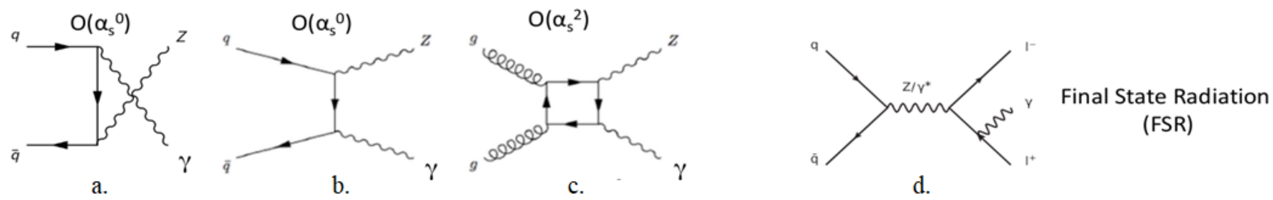

Figure 3: Feynman Diagram showing $Z+\gamma$ Production
a. & b. $q\bar{q} \to Z+\gamma$ c. $gg \to Z+\gamma$ d. Final State Radiation (FSR)

2 Approach

Following the method defined in the Ref [2], we define a variable $R(p_T)$ to be the ratio of the cross sections of $ZZ \to ll\nu\nu$ to $Z\gamma \to ll\gamma$ as a function of p_T.

$$R(p_T) = \frac{\sigma_{ZZ}(p_T)}{\sigma_{Z\gamma}(p_T)} \tag{1}$$

With the two processes being kinematically similar at high p_T, R depends on the coupling of the Z and γ to quarks. It should approach some value asymptotically.

The photon - quark and Z boson - quark couplings in the Standard Model are given by,

$$-ieQ_q\gamma^\mu \qquad \text{and} \qquad \frac{-ie}{2\sin\theta_W\cos\theta_W}\gamma^\mu(v_q - a_q\gamma_5) \tag{2}$$

respectively, where Q_q, v_q and a_q are respectively the electric, vector and axial neutral weak couplings of the quarks, and θ_W is the weak mixing angle. The cross sections are dependent on the matrix

[1] The branching fraction of Z to any one flavor of lepton is $\approx 3.4\%$, and to neutrinos is $\approx 20\%$.

elements squared, which contain factors of Q_q^2 for γ, or $(v_q^2 + a_q^2)/4\sin^2\theta_W \cos^2\theta_W$ for Z. There is a contribution due to the Z mass which appears in the internal propagators and phase space integration. This contribution becomes less important in the $p_T(\gamma) \gg M_Z$ region.

Thus, in the high p_T region, the Z and γ cross sections would be in the ratio

$$R_q = \frac{v_q^2 + a_q^2}{4\sin^2\theta_W \cos^2\theta_W * Q_q^2}. \tag{3}$$

Considering the contributions from both u and d flavor quarks,

$$R = \frac{Z_u \langle u\rangle + Z_d \langle d\rangle}{\gamma_u \langle u\rangle + \gamma_d \langle d\rangle} \tag{4}$$

Substituting $\sin^2\theta_W = 0.2315$, at moderate p_T values, $R \approx 1.4$[2].

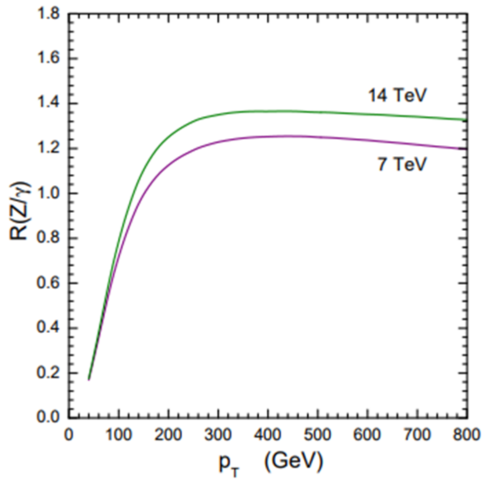

Figure 4: Ratio of the Z and γ p_T distributions [2]

This ratio R can be used as is for $ZZ \to ll\nu\nu$ and $Z\gamma \to ll\gamma$, as the contribution from the $Z \to ll$ is identically multiplied into the numerator as well as the denominator, and thus cancels out.

MCFM cross sections

A Monte Carlo program, MCFM v8.0 [3] at NLO is used to generate cross sections of $ZZ \to ll\nu\nu$ and $Z\gamma \to ll\gamma$ processes, with a selection of generator level cuts. The samples are generated with cuts on $E_{T,min}^{miss}$ for the ZZ process $p_{T,min}(\gamma)$ for the $Z + \gamma$ process. A ratio of these cross sections is taken to obtain the R distribution as a function of p_T. The uncertainty on R is calculated by varying several parameters at the generator level, such as the renormalization and factorization scales, the PDF sets used, photon fragmentation, etc. Effects of applying lepton cuts on the cross sections as well as the ratio, and the contributions of the $q\bar{q}$ and gg processes are also studied.

However, the MCFM generator only produces $Z \to ee$ instead of $Z \to ll$. Thus, this branching ratio needs to be accounted for to obtain the value of R.

$$R_{inc} = R * \frac{BR(Z \to ee)}{BR(Z \to ee) * BR(Z \to \nu\nu) * 2} \tag{5}$$

[2]Equations (3) and (4), as well as the value of R are taken from Ref [2]

3 Generator Parameters

The samples are generated using MCFM v8.0 for the following data points[3]

$$\text{For } ZZ \to ee\nu\nu : E_T^{miss} > \{50, 75, 100, 125, 150, 200, 250, 300, 400, 500\} \text{ GeV}$$
$$\text{For } Z(\to ee) + \gamma : p_T(\gamma) > \{50, 75, 100, 125, 150, 200, 250, 300, 400, 500\} \text{ GeV}$$

Table 1 lists the generator level settings used for the ZZ and $Z + \gamma$ processes. All lepton cuts are consistent with the ones used in the ATLAS Z+MET analysis.

Cuts	$ZZ \to ee\nu\nu$	$Z(\to ee) + \gamma$
Process ID	87	300
M_{ee}	$81 < M_{ee} < 101$ GeV	$81 < M_{ee} < 101$ GeV
$M_{\nu\nu}$	$81 < M_{\nu\nu} < 101$ GeV	-
Order	NLO	NLO
PDFset	CT14	CT14
$p_T^{\text{lead}}(e)$	> 30 GeV	> 30 GeV
$\eta^{lead}(e)$	< 2.5	< 2.5
$p_T^{\text{sublead}}(e)$	> 20 GeV	> 20 GeV
$\eta^{sublead}(e)$	< 2.5	< 2.5
$\Delta R(\gamma, e)$	-	0.7
Renormalization scale	91.187 GeV	91.187 GeV (M_Z)
Factorization scale	91.187 GeV	91.187 GeV (M_Z)

Table 1: Settings in input.DAT for MCFM

The constraint on M_{ee} in the case of $Z+\gamma$ suppresses the FSR process by ensuring that the lepton pair are from a Z decay only.

4 Results

Upon running the steering file with the parameters described above, the cross sections shown in Figure 5 are obtained. Throughout this analysis, this sample is the reference.

[3]MCFM does not generate $Z \to ll$ but $Z \to ee$. As electrons and muons have similar properties with the exception of mass, simply the branching fraction of $Z \to ee$ must be accounted for at a later stage.

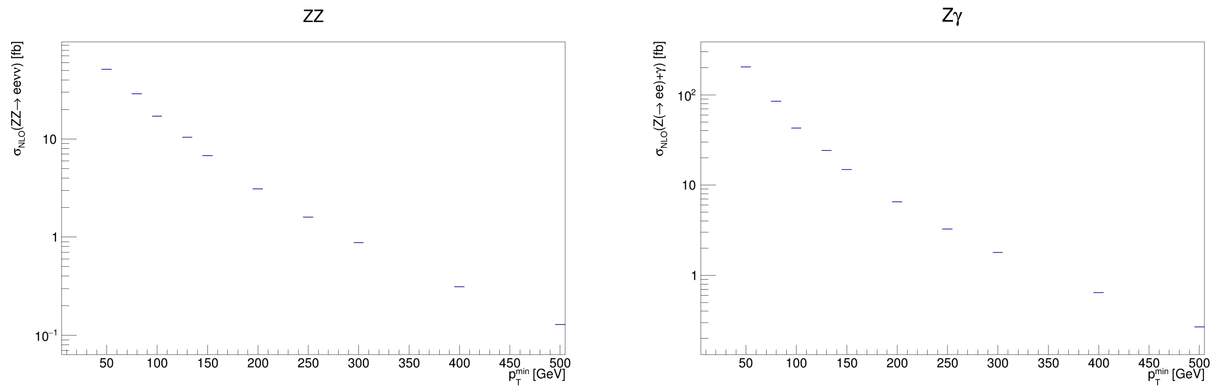

(a) $ZZ \to ee\nu\nu$ cross section

(b) $Z(\to ee) + \gamma$ cross section

Figure 5: Cross sections of ZZ and $Z + \gamma$ processes with the cuts as in Table 1. The Y axis is in $\log_{10}$ scale. The leptonically decaying Z boson decays to an e^+e^- pair. There is no flavor constraint on the neutrinos.

The ratio $R = \sigma(ZZ \to ee\nu\nu)/\sigma(Z\gamma \to ee\gamma)$ is shown in Figure 6

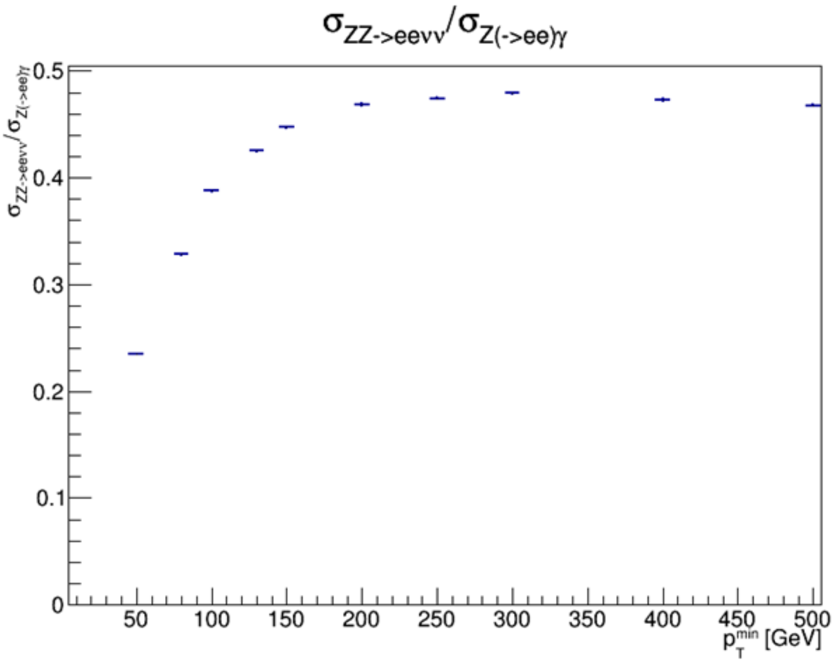

Figure 6: The transfer factor R as a function of p_T, taken as a ratio of plots 5a and 5b. The leptonically decaying Z boson decays to an e^+e^- pair.

The R value is observed to increase from ≈ 0.24 at 50 GeV to ≈ 0.47 at high p_T, where it is constant. When the branching ratio of Z boson decaying selectively to e^+e^-, or to $\nu\nu$, is accounted for as shown in Equation 5, the resulting ratio $R(p_T)$ is shown in Figure 7, which shows the ratio of $\sigma(ZZ)$ to $\sigma(Z\gamma)$, i.e. if the Z bosons do not decay further. The value of R is observed to increase from ≈ 0.61 at 50 GeV to ≈ 1.2 at high p_T.

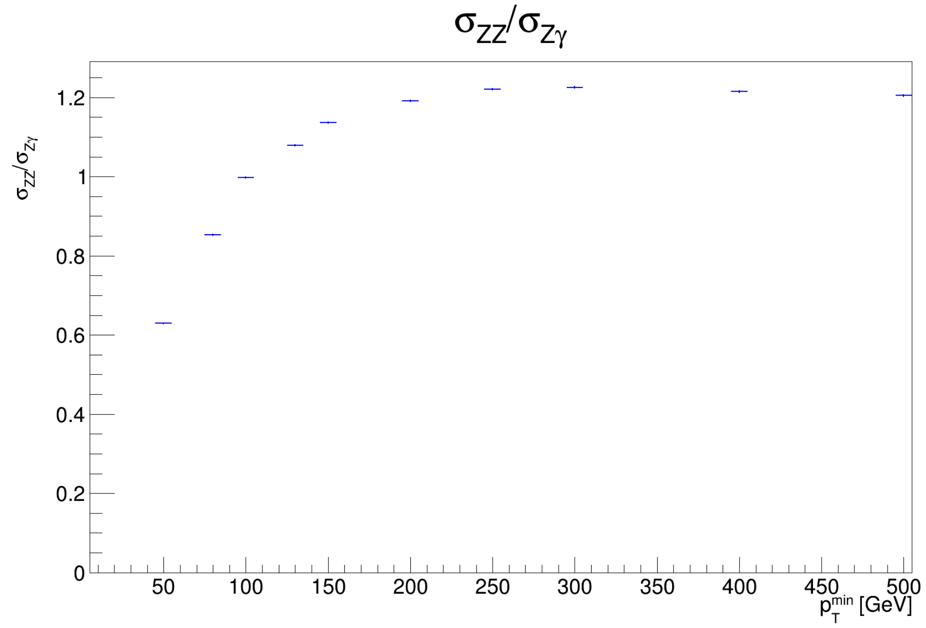

Figure 7: The transfer factor R as a function of p_T, adjusted for the $Z \to ee$ and $Z \to \nu\nu$ branching ratios. This shows the $R = \sigma(ZZ)/\sigma(Z\gamma)$, where the Z bosons do not decay.

Gluon-gluon processes contribute to 8.6% of the total cross section for the ZZ process and 2.5% of the $Z + \gamma$ process. Figure 8 shows the transfer factor R obtained from the gg process, as well as R from the $q\bar{q}$ and qg processes.

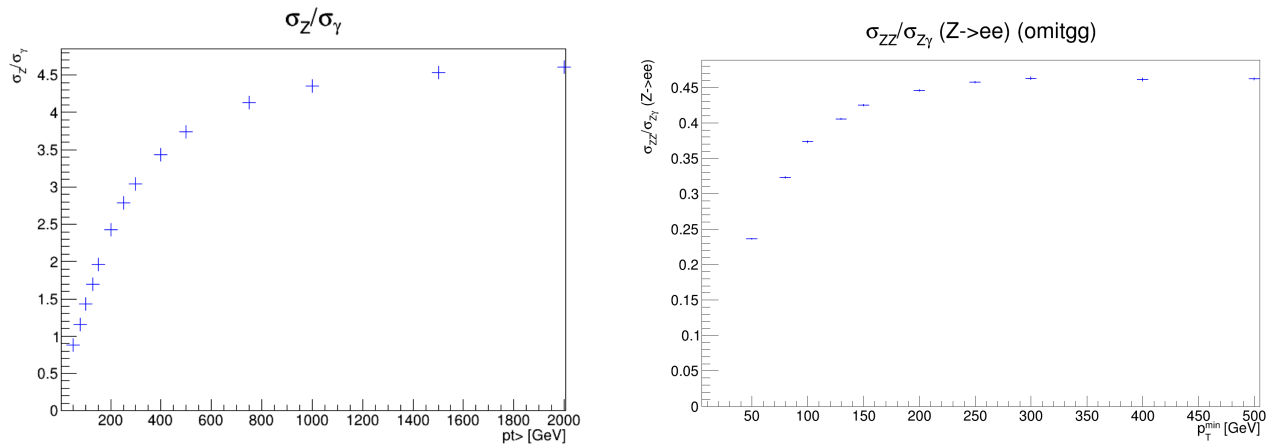

(a) $R_{gg}(p_T)$ as the ratio of $\sigma(gg \to ZZ)$ to $\sigma(gg \to Z\gamma)$ only, Figure 2c and 3c.

(b) $R_{q\bar{q}/qg}$ calculated from the contribution of $q\bar{q}$ and qg to ZZ and $Z\gamma$ processes.

Figure 8: The ratio $R(p_T)$ from the contributing quark and gluon processes. The Z bosons decay further to e^+e^- for the leptonic Z boson, or $\nu\nu$ for the invisibly decaying Z boson.

The R_{gg} distribution is observed to approach an asymptotic value at a much higher $p_T = 1.5$ TeV. The shape and scale of the R_{gg} distribution (Figure 8a) remain to be understood, as they differ from Figure 6.

4.1 Effect of Lepton Cuts

To check the effects of lepton cuts on the ratio, samples with the same parameters as those in Table 1 are generated. However, we relax the cuts on leptons. Both the leading and subleading lepton should have $p_T > 5$ GeV, and $\eta < 10$. In the lower p_T regions, the cross section falls by nearly half in both processes. The ratio is affected by up to 15% as seen in Figure 9, and therefore for all following studies the lepton cuts are applied as they emulate the experimental cuts needed in the analysis.

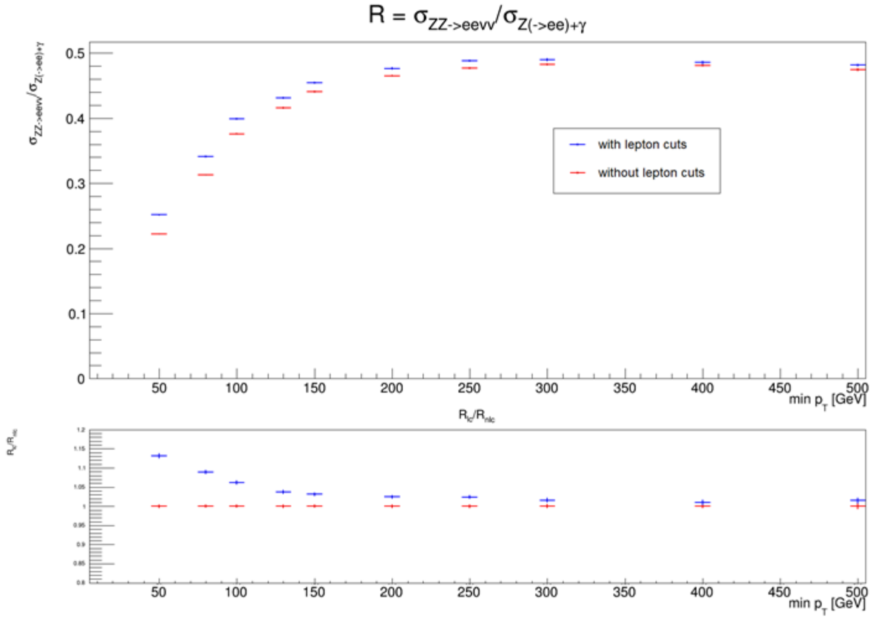

Figure 9: Comparison of reference the R distribution to the R distribution without lepton cuts

4.2 Uncertainty from Scale Variation

The renormalization and factorization scales are arbitrary parameters that address the UV and IR divergences respectively that arise while calculating cross sections. They are important when considering higher order effects in QCD. To obtain the uncertainties associated to these scales, the renormalization (μ_R) and factorization (μ_F) scales are each varied by a factor of 2 in either direction from the central value, $M_Z = 91.187$ GeV, to obtain the uncertainty as shown in Figure 10.

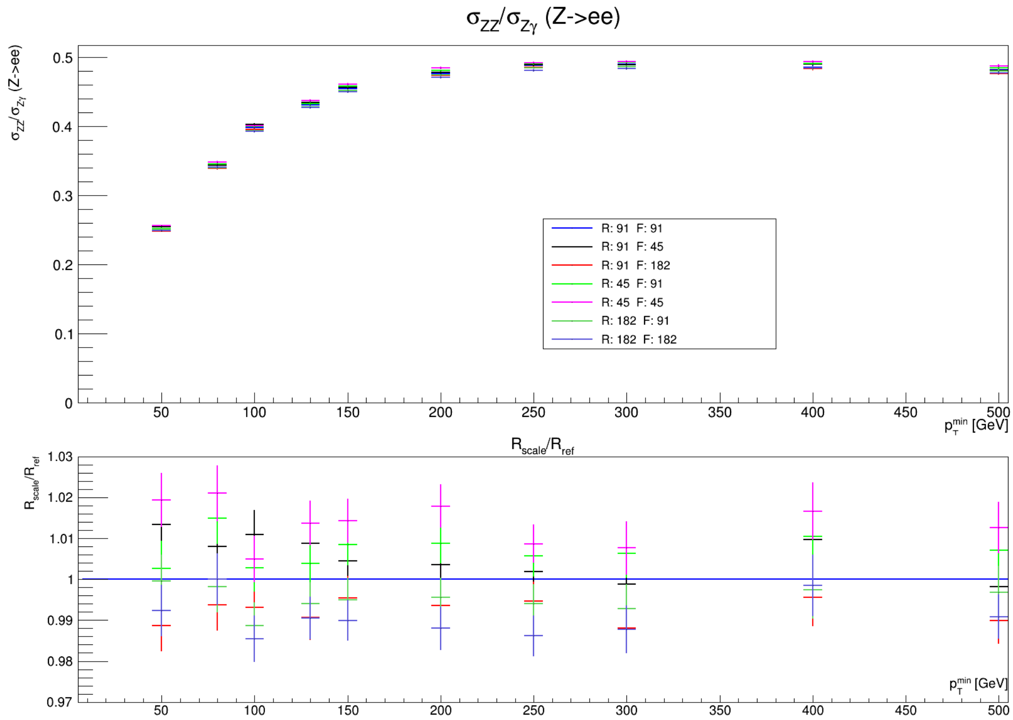

Figure 10: The ratio $R(p_T)$ for various choices for μ_R (R) and μ_F (F). The bottom panel shows the relative - with respect to the reference (R: 91, F: 91) for each scale. The uncertainties are statistical

The uncertainty due to the variation of scales around $R = 0.398$ is $\pm \approx 2\%$ for all p_T. The contributions from the gg subprocess separately from the $q\bar{q}$ and qg subprocesses are shown in Figure 11.

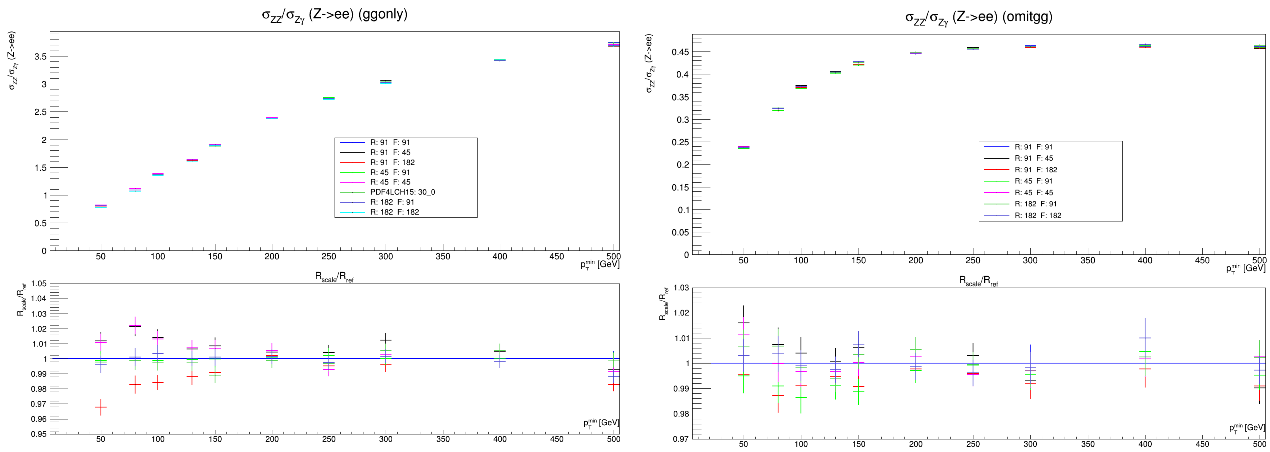

(a) R_{gg} from gg subprocess only

(b) $R_{q\bar{q}/qg}$ from $q\bar{q}$ and qg subprocesses

Figure 11: The ratio $R(p_T)$ for various choices for μ_R (R) and μ_F (F) for the gg and qg+$q\bar{q}$ subprocesses separately. The bottom panel shows the relative difference with respect to the reference (R: 91, F: 91) for each scale. The uncertainties are statistical.

Variations of up to 3% are seen at low pt while at high pt the differences are below 1% for the plots show in Figures 10 and 11

4.3 Uncertainty from PDF variation

The PDF set used for reference is the `CT14`[4] PDF set. The uncertainty on the PDFs is studied by using the 30 variations provided by the `PDF4LHC15` set[5], constructed from the combination of `CT14`,`MMHT14`[6] and `NNPDF3.0`[7] PDF sets. These sets are provided by LHAPDF6[8]. `PDF4LHC15` provides a set of variations that include those determined by different groups (MSTW, CTEQ and NNPDF). The group used here is `PDF4LHC15_nlo_30`, consisting of 30 PDF sets. While the most accurate uncertainties are given by `PDF4LHC15_nlo_100` sets, `PDF4LHC15_nlo_30` is used here for a faster, reasonably accurate estimate of the uncertainties.

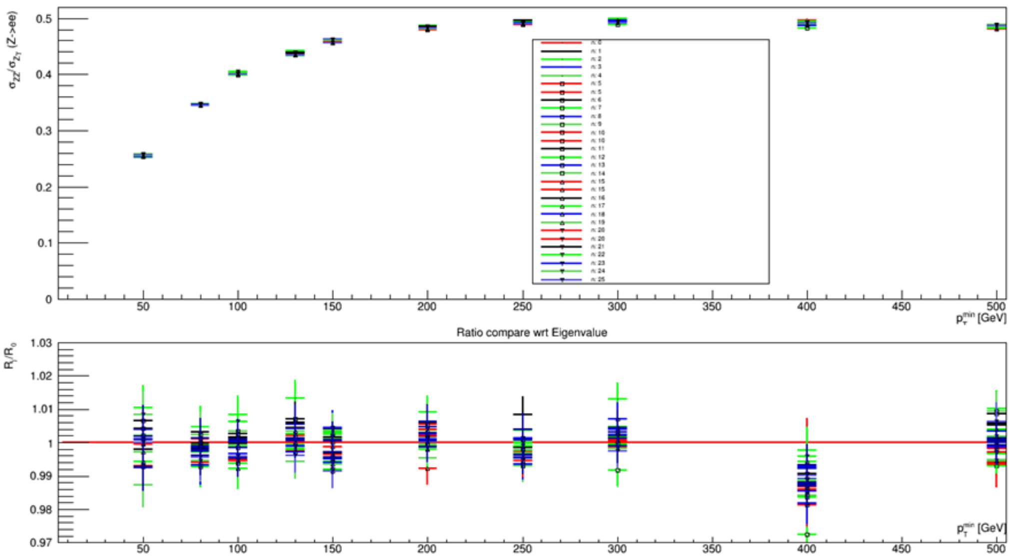

Figure 12: The ratio $R(p_T)$ for each of the 30 PDF sets in `PDF4LHC15_nlo_30`. The bottom plot shows the relative differences of sets 1-30, with respect to set 0 which is taken as the central value.

Fig.12 shows the comparison of the ratio $R(p_T)$ from the 30 member sets of `PDF4LHC15_nlo_30`. To measure the uncertainty due to these 30 sets, the relation as stated in Equation 20 in Ref [5] is used:

$$\delta^{PDF}\sigma = \sqrt{\sum_{k=1}^{N_{mem}} (\sigma^{(k)} - \sigma^{(0)})^2} \tag{6}$$

where N_{mem} is the number of member sets in the group, in this case, 30. The R distribution obtained from the `PDF4LHC15_nlo_30` set is compared to the reference distributions from `CT14`, as shown in Figure 13:

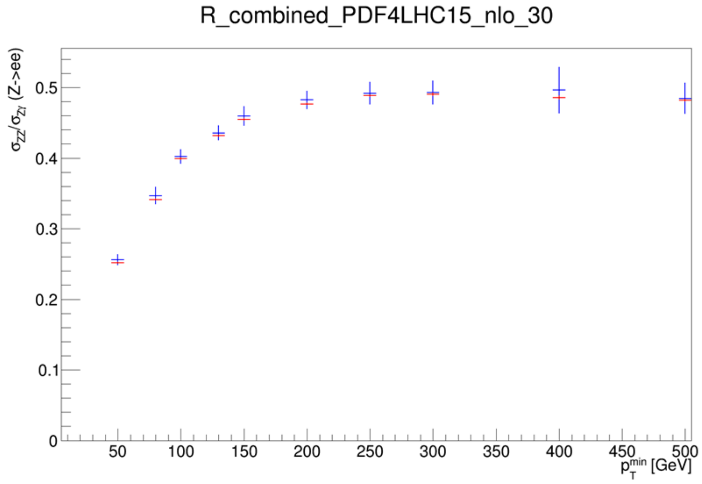

Figure 13: The ratio $R(p_T)$ of the `PDF4LHC15_nlo_30` with combined uncertainties as given by Equation 6 (blue), to the reference constructed from the PDF set `CT14` (red).

Figure 13 shows a comparison between the central value of the sets in `PDF4LHC15_nlo_30` with the combined uncertainties, and the reference PDF set `CT14`. The combined uncertainty around $R \approx 0.40$ is $\pm 2.55\%$ at 100 GeV. The R distributions drawn from the two PDF sets agree to within the uncertainty bounds.

4.4 Photon Fragmentation

The $Z\gamma \rightarrow ll\gamma$ process may contain photons that arise from the hadron showers. It is therefore important to isolate the prompt photon from hadronic activity. This reduces unwanted background from pion decays, or fragmentation processes.

Experimentally, photon isolation is implemented with the following cuts:

$$\sum_{\in R_0} E_T(\text{had}) < \epsilon_h p_T^\gamma \qquad \text{or} \qquad \sum_{\in R_0} E_T(\text{had}) < E_T^{max} \tag{7}$$

limiting the transverse hadronic energy $E_T(had)$ in a cone of size $R_0 = \sqrt{\Delta\eta^2 + \Delta\phi^2}$ around the photon, to some fraction of the photon p_T, or some fixed small cut-off.

The smooth cone isolation method of Frixione [9] is an alternative isolation procedure, which simplifies calculations by avoiding fragmentation contribuitions. The following isolation prescription is applied to the photon:

$$\sum_{R_{j\gamma} \in R_0} E_T(\text{had}) < \epsilon_h p_T^\gamma \left(\frac{1 - \cos R_{j\gamma}}{1 - \cos R_0} \right)^n . \tag{8}$$

where $R_{j\gamma}$ is the separation of the photon and the j^{th} hadron. This requirement constrains the sum of hadronic energy inside a cone of radius $R_{j\gamma}$, for all separations $R_{j\gamma}$ less than a chosen cone size R_0. This prescription allows soft radiation inside the photon cone, but collinear singularities are removed. The smooth cone isolation is infrared finite, thus fragmentation contributions do not need

to be included.
Smooth isolation is difficult to implement experimentally, however, both methods are explored here, as the different may give a handle on the effects of fragmentation.

In this analysis, R_0 is chosen to be 0.4. The central value is chosen to be from the sample using smooth cone isolation (Frixione) with $\epsilon_h = 0.075$ and $n = 1$. The comparisons with variations to these two variables is shown in Figure 14.

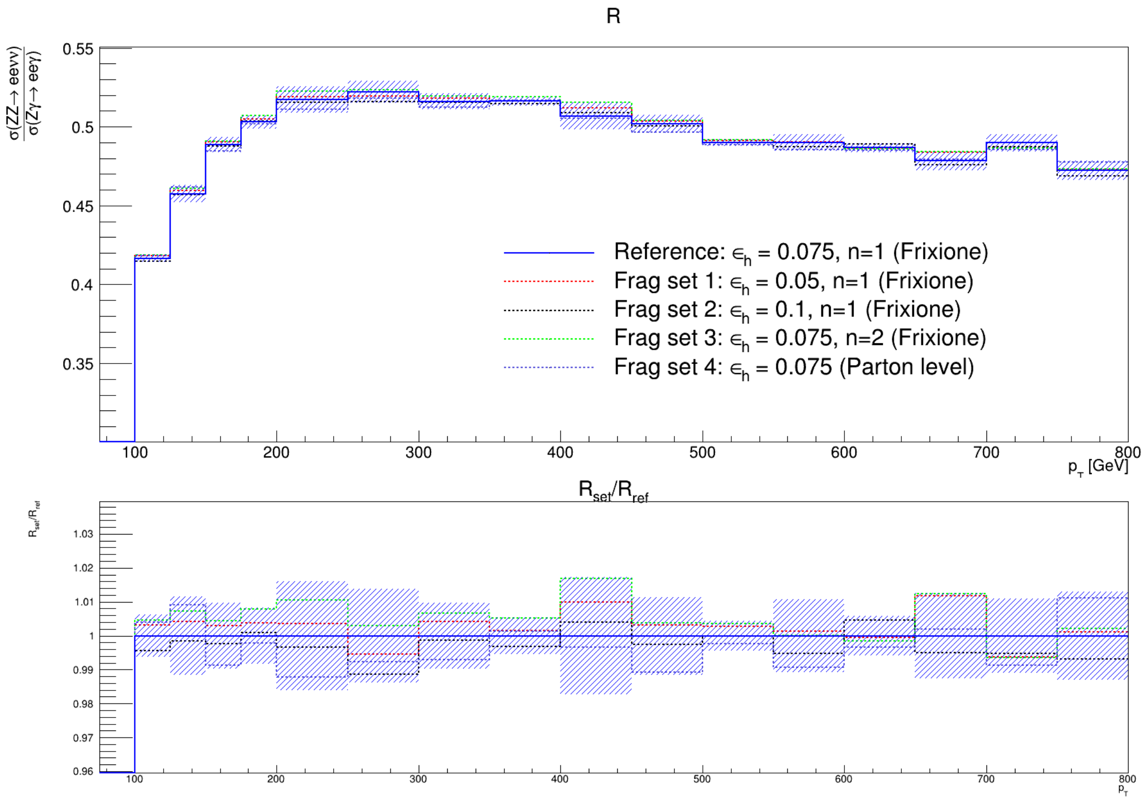

Figure 14: R distribution as a function of p_T, showing the uncertainty due to variation of photon isolation parameters ϵ_h and n in the smooth cone isolation procedure (Frixione), and ϵ_h in the photon isolation procedure. The lower panel shows the relative deviation of the varied sets from the central value, as well as the uncertainty band.

The uncertainty is calculated in the following manner:

$$\begin{aligned} \delta R_i &= |R_i - R_{ref}| \qquad\qquad i \in (1,2,3,4) \\ \delta R &= \sqrt{\max_{i=1,2,3}(\delta R_i)^2 + (\delta R_4)^2} \end{aligned} \tag{9}$$

as the Frixione procedure and the experimental photon isolation procedure are assumed to be independent.
An uncertainty is $< 2\%$ over the whole range, which has been extended up till 800 GeV.

5 Conclusion

We propose a new method to estimate the $ZZ \to ll\nu\nu$ contribution to the $ll + E_T^{miss}$ signal from $Z\gamma \to ll\gamma$ data, using a transfer factor R. We quantify the uncertainty from sources such as renormalization and factorization scales and different PDF distributions.
From these, we observe that at high p_T, the value of R approaches 0.47, while at $p_T = 100$ GeV, $R = 0.40$. The uncertainty is quantified $\approx 2\%$ from scale variation, and $\approx 2.55\%$ from PDF variation. The uncertainty due to photon fragmentation is $< 2\%$ for the full p_T range, up to 800 GeV.

Acknowlegements

This work was conducted under the patient supervision of Dr. Beate Heinemann. In addition to her guidance and advice, I had the help of Dr. Yee Chinn Yapp, who helped me work on streamlining the presentation of this work; Dr. Pieter Everaerts, who helped me debug the code and understand the physics better, and Dr. Sarah Heim, whose office is close enough to mine that I could bother her for the tiniest of details.

Bibliography

[1] *Search for an invisibly decaying Higgs boson or dark matter candidates produced in association with a Z boson in pp collisions at $\sqrt{s}$ = 13 TeV with the ATLAS detector*
ATLAS Collaboration
`arXiv:1708.09624`

[2] *Using $\gamma+$ jets to calibrate the Standard Model $Z(\rightarrow \nu\nu)+$ jets background to new processes at the LHC*
S. Ask, M. A. Parker, T. Sandoval, M. E. Shea, W. J. Stirling
Cavendish Laboratory, University of Cambridge, CB3 0HE, UK; 2011
`[arXiv:1107.2803]`

[3] *Monte Carlo for FeMtobarn processes (MCFM) v8.0 User Manual*
John Campbell, Keith Ellis, Walter Giele, Ciaran Williams
`https://mcfm.fnal.gov/`

[4] *New parton distribution functions from a global analysis of quantum chromodynamics*
Sayipjamal Dulat, Tie Jiun Hou, Jun Gao, Marco Guzzi, Joey Huston, P. Nadolsky, Jon Pumplin, Carl Schmidt, Daniel Stump, C. P. Yuan
`arXiv:1506.07443`

[5] *PDF4LHC recommendations for LHC Run II*
`[arXiv:1510.03865]`

[6] *Parton distributions in the LHC era: MMHT 2014 PDFs*
L. A. Harland-Lang, A. D. Martin, P. Motylinski, R. S. Thorne
`arXiv:1412.3989`

[7] *Parton distributions for the LHC Run II*
The NNPDF Collaboration: Richard D. Ball, Valerio Bertone, Stefano Carrazza, Christopher S. Deans, Luigi Del Debbio, Stefano Forte, Alberto Guffanti, Nathan P. Hartland, Jose I. Latorre, Juan Rojo, Maria Ubiali
`arXiv:1410.8849`

[8] *LHAPDF6: parton density access in the LHC precision era*
Andy Buckley, James Ferrando, Stephen Lloyd, Karl Nordstrom, Ben Page, Martin Ruefenacht, Marek Schoenherr, Graeme Watt
`arXiv:1412.7420`

[9] *Isolated photons in perturbative QCD*
S. Frixione
Phys. Lett.B429(1998)369–374, hep-ph/9801442

[10] *ATHENA reference*
`ATHENA reference`

[11] POWHEG BOX - ZZ,WZ and WW production

- **P. Nason**
  JHEP 0411 (2004) 040, hep-ph/0409146
- **S. Frixione, P. Nason and C. Oleari**
  JHEP 0711 (2007) 070, `arXiv:0709.2092`
- **S. Alioli, P. Nason, C. Oleari and E. Re**
  JHEP 1006 (2010) 043, `arXiv:1002.2581`
- *ZZ, WZ and W+W- production, including Gamma/Z interference, singly resonant contributions and interference for identical leptons*
  T. Melia, P. Nason, R. Rontsch, G. Zanderighi
  JHEP 1111 (2011) 078, `arXiv:1107.5051`
- *W+W-, WZ and ZZ production in the POWHEG-BOX-V2*
  P. Nason and G. Zanderighi
  Eur.Phys.J. C74 (2014) 2702, `arXiv:1311.1365`

[12] *PYTHIA 8.1*
T. Sjöstrand, S. Mrenna and P. Skands
JHEP05 (2006) 026, Comput. Phys. Comm. 178 (2008) 852.

[13] *New parton distributions for collider physics* **Hung-Liang Lai, Marco Guzzi, Joey Huston, Zhao Li, Pavel M. Nadolsky, Jon Pumplin, C.-P. Yuan** `arXiv:1007.2241`

[14] *Parton distributions for the LHC*
A.D. Martin, W.J. Stirling, R.S. Thorne, G. Watt `arXiv:0901.0002`